INTERNAL FRICTION PHENOMENA ASSOCIATED WITH DIFFUSIONLESS PHASE TRANSFORMATIONS IN ALLOYS

K. Sugimoto

JOURNAL DE PHYSIQUE
Colloque C5, supplément au n°10, Tome 42, octobre 1981 *page* C5-971

INTERNAL FRICTION PHENOMENA ASSOCIATED WITH DIFFUSIONLESS PHASE TRANSFORMATIONS IN ALLOYS

K. Sugimoto

Department of Metallurgy, Kansai University, Senriyama-higashi, Suita, Osaka 564, Japan

Abstract Internal friction and ultrasonic attenuation peaks associated with diffusionless phase transformations in alloys, such as thermoelastic martensites and others, were reviewed. They were discussed from the stand point of (1) Understanding the mechanism of the phase transformations and (2) Developing new alloy materials of high damping capacity for application to noise and vibration abatement. Phase transformation peaks, a twin-boundary relaxation peak, and a Zener peak were identified in Mn-Cu, Mn-Ni, In-Tl, In-Cd, Au-Cd, Ti-Ni, Cu-Al-Ni, Cu-Al-Mn, and Cu-Zn-Al alloys, respectively.

1. Introduction Coupled phenomena of elasticity with other physical properties, such as magnetism, electricity and others, have been known for a long time. The magnetoelastic effect is responsible for the high damping in some ferromagnetic materials. It is called magnetoelastic hysteresis damping and has been studied intensively by many workers. The piezoelectric effect is responsible for the electric polarization in ionic crystals under applied stress. Internal friction phenomena due to the magnetic and electric effects have been reported by many workers. However, the interaction of elastic energy with thermal energy is known only by the thermoelastic effect in metals and alloys. It is responsible for the resisting force of dislocations to motion through the lattice. When a region of expansion or contraction around a dislocation moves through the lattice, it will be accompanied by an adiabatic volume change that results in a temperature change. In most metals and alloys this effect is not very large. The micro and macro-thermal flow in a specimen vibrating transversely will contribute to the thermoelastic damping, which is usually very small compared with other damping phenomena. This is because elasticity originates from the potential energy of the crystal atoms in most metals and alloys, and hence the coupling between thermal and elastic energies can be only possible within the limit of thermal expansion of the lattice, which is not very large. Such an elasticity can be called "energy **elasticity** ".

The large elastic deformation in rubber can be explained in terms of "entropy elasticity". In this material the energy ealsticity is so

small that it can be neglected, while the change in distance and angle between the molecular chains under applied stress will contribute to the elastic deformation. It is a change in entropy and hence it is called entropy elasticity. The entropy decreases when stressed and increases again when unloaded. Equation (1) shows that the force necessary to elastically deform a material of length x consists of the two **elasticity** terms,

$$F = \left(\frac{dU}{dx}\right)_T - T\left(\frac{dS}{dx}\right)_T \qquad (1)$$

where F is the force, U is the internal energy, S is the entropy, and T is the temperature of the material.

In some alloys called thermoelastic martensites the effect of the temperature on elasticity is so large that it cannot be understood in terms of the energy elasticity. The martensite phase contains as a result of the self-accomodation internal faults such as twins, stacking faults or even dislocations. Rearrangement of these internal faults may contribute to a kind of entropy elasticity which results in an anomalously large thermal expansion and internal friction. The purpose of the present paper is to describe typical experimental results on internal friction and elastic constant measurements in alloys with the thermoelastic martensite transformation and to discuss them on the basis of physical metallurgy of martensite in high damping alloys.

2. Mn-Cu Alloys Alloys containing 40 wt% Mn or more are known to be very high damping when quenched from the γ-phase range or aged after quenching (see Fig.4). The internal friction originates from the phase transformation from fcc to fct at around the Neél-temperature. Although it is closely connected with the antiferromagnetic ordering in the fcc phase, it is a kind of martensitic transformation because it goes in a diffusionless and shear-like way. In order to reduce the total strain energy the fct martensite phase is accompanied by microtwin boudaries of the $\{101\}$-type. These make the material very high damping. Stress relaxation across the twin boudaries is shown in Fig.1 (1,2,3) and Fig.2 (4). A phase transformation peak B is observed together with the twin-boundary relaxation peak A in Fig.3 (5). It is remarkable to see that the phase transformation peak is accompanied by a large elastic anomaly as shown in Fig.5 (6). The γ-phase Mn-Cu alloy is the only example where the phase transformation peak and the twin-boundary relaxation peak have been both found clearly. Fig.6 will give

examples of the peak separation (7).

The transformation fcc⇌fct does not occur in alloys with less than 70 at% Mn as the Neél-temperature falls down to 0K as shown in Fig.4. If the alloy is aged at 375°C for the time given in Fig.6 after quenching from 850°C, the alloy containing 44.6 wt% Mn becomes antiferromagnetic and the fcc⇌fct transformation peak is observed at increasing temperatures with increase in ageing time. Fig.7 illustrates the change in the internal friction spectrum of the quenched and aged alloy with lower Mn-content (7). The low temperature peaks P_1 and P_2 are not well known yet, whereas P_3 and P_4 are the twin-boundary relaxation peak, respectively. It is interesting to know that the internal friction profile has changed to a great extent depending on the position of the transformation peak shown by arrows in Fig.7.

The above experiments were carried out at frequencies of about 1 kHz. The results in Fig.8 are obtained at a frequency of 5 MHz by means of an ultrasonic attenuation measurement with pulse-echo method in a single crystal specimen of a 37.2 wt% Mn-Cu alloy (8). The specimen was solution-treated at 720°C followed by quenching and then aged at 425°C for 4 hr, so that the phase transformation fcc⇌fct occurs at around 300K. It was concluded that the twin-boundary relaxation peak can be thermally activated, the activation energy being about 5.15×10^4 J/g atom. It is interesting to confirm that the temperature of the phase transformation peak does not depend on the frequency, but only on the history of heat treatment. Fig.9 shows a similar phase transformation peak observed in a 77.7 at% Mn-Ni alloy specimen quenched from 950°C. (9).

3. <u>In-Tl Alloys</u> It is known that In-rich alloys undergo a fcc⇌fct phase transformation which occurs in a diffusionless and shear-like way. Fig.10 shows examples of the internal friction peaks associated with the phase transformation (10). Peaks occurring at temperatures slightly below the M_s-temperature (the starting temperature of the martesite transformation) are seen in curves (a), (b), and (c). In an alloy with 25 at% Tl a Zener relaxation peak was observed as shown by curve (c) in Fig.10.

The height of the phase transformation peaks was smaller when the frequency was higher. There was a slight temperature hysteresis between the cooling and heating curves. It was concluded that the phase transformation peak was amplitude-dependent as shown in Fig.11 (10). The same transformation peaks were reported by use of ultrasonic attenuation measurement in single crystals as shown in Fig. 12 (11). Almost the same peaks were reported on In-Cd alloys (12).

4. Au-Cd Alloys The β-phase Au-47.5 at% Cd alloy has an ordered CsCl (B_2) type structure above 350K. Upon cooling in the vicinity of 333K, this cubic phase transforms martesitically to the orthorhombic β' structure with four atoms in a unit cell. Fig.13 shows the change in the ultrasonic sound velocity C_L and attenuation coefficient α with the phase transformation (13). The same change in Young's modulus E (see Fig.14), shear modulus, Poisson's ratio, and adiabatic compressibility K_s (see Fig.15) was observed. It is interesting to know that the serrations observed on the curves of the attenuation coefficient in Fig.13 apparently represent the multiple-interface mechanism of the transformation (13). The bulk effect is reflected on the elastic anomalies, while the ultrasonic attenuation is more sensitive in the detection of the formation of the martensite plates and its twinned boundaries.

5. Ti-Ni Alloys Fig. 16 shows a sharp internal friction peak and the elastic anomalies reported in an early work done at about 1 Hz (14). Ultrasonic attenuation measurements on polycrystalline TiNi specimens has made clear that the sharp attenuation peak and the velocity anomaly may be caused by a similar mechanism as the "Akhieser effect" in ferroelectric materials (see Fig.18) (15). Fig.17 shows the anomaly in the thermal expansion coefficient of the same alloy in the vicinity of the martesnite transformation temperature. It should be mentioned that careful experiments on internal friction of single cyrstal specimens with a well-known thermal history must be carried out in order to make clear the mechanism of the peak. The high damping behavior of the Ti-Ni alloys is, therefore, not so well-known as the famous "shape-memory effect" of the same alloy.

6. Cu-Al-Ni Alloys The β-phase Cu-Al-Ni alloy has an ordered bcc (DO_3) structure above the transformation temperature which are usually in the range from -150 to 100°C according to the Al-content. On passing through the transformation temperature, the cubic phase transforms to the orthorhombic γ_1' (or β_1' when the Al-content is smaller) martensite phase. Fig.19 shows the change in internal friction, Young's modulus, and the shape change accompanied by the phase transformation (or anomalous thermal expansion due to martensite transformation) in a single crystal specimen of a Cu-14.5 wt% Al-4.4 wt% Ni alloy (18).

The transformation temperature shown at the top of the figure were determined by electric resistivity measurements. It was confirmed that the internal friction consists of the three components. They are

(1) Low internal friction at temperatures above M_s (or A_f on heating), originating from movements of dislocations in the β_1-phase, (2) Very sharp internal friction peak in the transformation range between M_s and M_f (or A_s and A_f on heating), originating from movements of interfaces between the martensite and the β_1-phases, and (3) High internal friction at temperatures below M_f(or A_f on heating), originating from movements of the twin faults or martensite boundaries in the martensite phase (16, 17, 18). Ultrasonic attenuation peak at the transformation temperature was found in single crystal specimens of a Cu-13.0 wt% Al-3.6 wt% Mn alloy (19). It is still not well known why a twin-boundary relaxation peak cannot be found in these Cu-base alloy martensites with internal twin faults.

7. Cu-Zn-Al Alloys The β_1-phase of the Cu-Zn-Al alloys with ordered structure transforms martensitically from a bcc to an orthorhombic 9R or 18R structure (20). Internal friction peaks and the elastic anomalies have been reported by several workers. Fig.20 shows the effect of room-temperature ageing after quenching from the β-phase range on the internal friction peaks. It shows also the effect of heating (or cooling) cycle on the peak shape. It was pointed out that the thermomechanical history could give rise to an enhanced effect on the interface mobility and also on the martensite boundary mobility, thus producing a drastic change in the peak shape as shown in Fig.20.

The movement of martensite boundaries was responsible for the damping at high stress levels, while the movements of dislocations was responsible for the damping at low stress levels (20). The very sharp internal friction peak in Fig.22 obtained after 10 oscillations at a temperature of measurement completely disappeared in Fig.21, which was taken after 120 oscillations at the same temperature (21). This is in a sense consistent with the disappearence of the internal friction peak in Sample 2 which has been air-cooled from the β-range (22). Very small particles of the precipitated α-phase (or even Cu-rich zones since no precipitates could be seen under optical microscope) may impede the motion of the interfaces and hence reduce the internal friction peak as seen in Fig.24.(22). Fig 25 confirms the fact that the transformation in Sample 2 goes more slowly than in Sample 3 which has been water-quenched. Sample 1 is as hot-forged and has no martensite peak.

8. Conclusions It should be mentioned that the process of the martensitic transformation (or reverse transformation on heating) can be

well detected by measuring internal friction peak and the elastic anomalies. They are ,therefore, one of the best method for analysing the mechanism of the martensite transformation. if they are measured simultaneously with electric resistivity change (22. 23). Internal friction or attenuation peaks due to phase changes in some oxides has also been investigated (24). The effect of elastic anisotropy on the lattice dislocations and internal friction was discussed (see Fig.23) (25).

The effects of thermal history, cooling (or heating) rate, and measuring time on the internal friction peaks were discussed and the possibility of applying internal friction method to investigate the mechanism of the martensite (or reverse) transformations was pointed out. Several metallurgical aspects important for developing new high damping alloy materials with martesite phase have been suggested and discussed referring to the previous review papers (26, 27, 28).

References

(1) F.T. Worrell:J. Appl. Phys., 19(1948),927.
(2) C.Zener:*Elasticity and Anelasticity of Metals*, Chicago(1948),159.
(3) A.Siefert and F.T. Worrell:J. Appl. Phys., 22(1951),1257.
(4) T.Aoyagi and K.Sumino:phys. stat. soli., 33(1969),317 & 327.
(5) K.Sugimoto. T.Mori and S.Shiode:Met. Sci. J.,7(1973),103.
(6) K.Sugimoto and T.Mori:Proc. ICIFUAS-5, Aachen, (1973),418.
(7) K.Sugimoto and K.Mizutani:J. Japan Inst. Met., 39(1975),503.
(8) K.Sugimoto and K.Ohta:Proc. ICIFUAS-6, Tokyo(1977),725.
(9) N.Honda,Y.Tanji and Y.Nakagawa:J.Phys. Soc. Japan, 41(1978),1931.
(10) M.E.DeMorton:J. Appl. Phys., 40(1969), 208.
(11) D.J.Gunton and G.A.Saunders:Solid State Comm.,14(1974),865.
(12) M.R.Madhava and G.A.Saunders:Phil. Mag.,36(1977),777.
(13) Y.Gefen and R.Rosen:Phil. Mag.,26(1972),727.
(14) R.R.Hasiguti and K.Iwasaki:J.Appl. Phys.,39(1968), 2182.
(15) N.G.Pace and G.A.Saunders:Solid State Comm., 9(1971),331.
(16) I.A.Arbuzova, V.S.Gavrilyuk and L.G.Khandros:Fiz.met.metalloved., 27(1969),1126.
(17) V.S.Postonikov, I.M.Sharshakov and V.G.Komarov:Fiz.met.metalloved. 33(1972),222.
(18) K.Sugimoto,T.Mori, K.Otsuka and K.Shimizu:Script.Met.,8(1974)1341.
(19) K.Sugimoto, S.Yoshioka and K.Ohta:preprint for 84th Spring Meeting of Japan Inst.Met., April 1979,Tokyo, p.47 (in Japanese).
(20) W.Dejonghe, L.Delaey, R.DeBatist and J. van Humbeeck:Met.Sci., 10(1977),523.
(21) M.Morin, G.Guenin,S.Etienne and P.F.Gobin:Trans. JIM,22(1981)1.
(22) K.Sugimoto, Y.Nakamura and S.Komatsu:preprint for 88th Spring Meeting of Japan Inst. Met., April 1981, Tokyo, p.106(in Japanese).
(23) K.Sugimoto, Y.Nakamura and L.Delaey:these Proceedings, p.
(24) N.Igata,K.Domoto and R.R.Hasiguti:J.Phys. and Chem. Sol.,31(1970), 1883.
(25) O.Mercier and K.N.Melton:Proc. ICIFUAS-6,Tokyo(1977), 345.
(26) Discussion:*Physical Metallurgy of Alloys of High Damping Capacity*, J.Inst.Met., 93(1964),546.
(27) K.Sugimoto:Mem. Sci. & Ind. Res., Osaka Univ.,35(1978),31.
(28) N.Nakanishi:*Elastic Constants as They Relate to Lattice Properties and Martensite Formation, Progress in Metal Science*,Vol.24(1980), Pergamon, p.143/265.

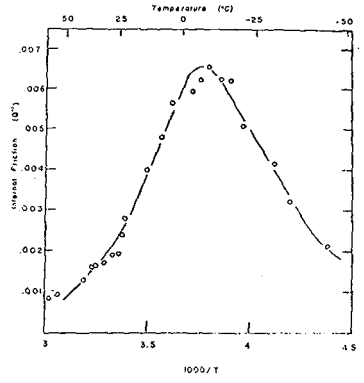

Fig.1 Stress relaxation across twin boundaries observed in an alloy 88 at%Mn-12 at%Cu quenched from 925°C to room temperature (1, 2, 3).

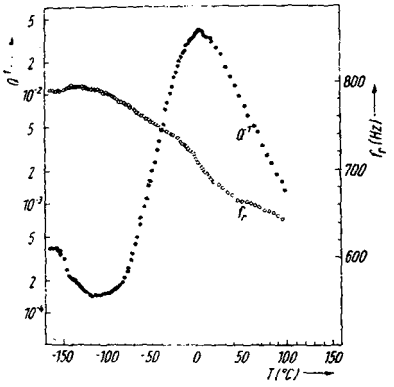

Fig.2 Internal friction and resonance frequency as a function of temperature in an alloy 89 at%Mn-11 at%Cu quenched form 950°C into ice-water (4).

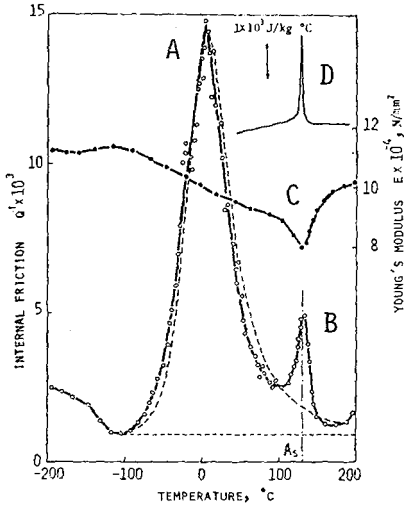

Fig.3 Twin-boundary relaxation peak A and phase transformation peak B with the corresponding modulus anomaly C in an alloy 88.26 wt%Mn-11.74 wt%Cu quenched from 900°C to room temperature. Anomaly in specific heat is shown in D (5, 6).

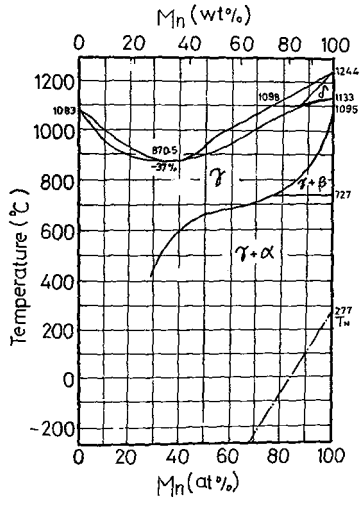

Fig.4 Equilibrium phase diagram for the binary system Mn-Cu.

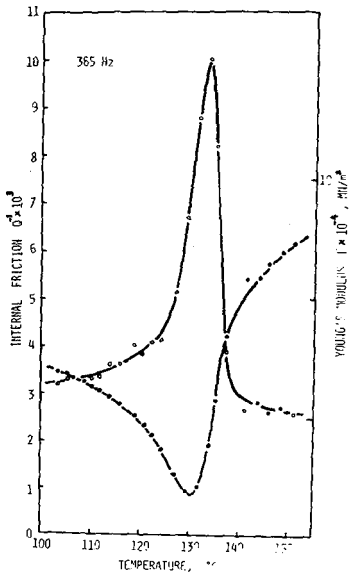

Fig.5 Enlarged phase transformation peak and the modulus anomaly of Fig.4 (6).

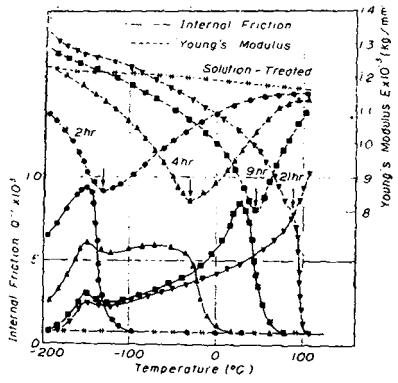

Fig.6 Change in internal friction and Young's modulus in an alloy 55.4 wt%Mn-44.6 wt%Cu with ageing time from 2 hr to 21 hr after quenching form 850°C (7).

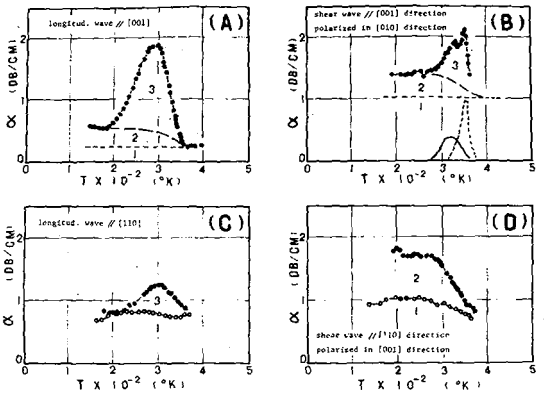

Fig.8 Ultrasonic attenuation coefficient of quenched (open circle) and aged (solid circle) crystals as a function of temperature. (1) background attenuation, (2) attenuation due to the movement of defects in the fct-phase, and (3) attenuation peak associated with the {101} - twin boundaries and the fcc⇌fct phase transformation (8).

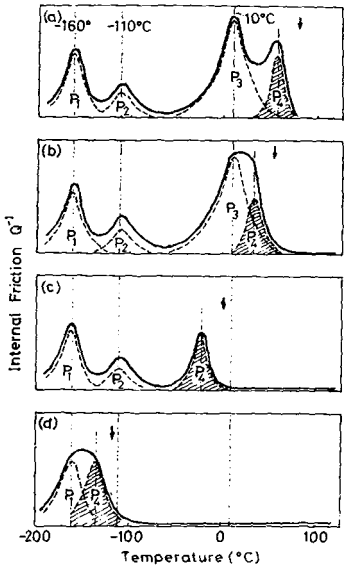

Fig.7 Schematic illustration showing the effect of ageing time on the internal friction behavior of the same alloy as in Fig.6. Ageing time ;2 hr (d), 4 hr (c), 9 hr(b), 21 hr (a), respectively (7).

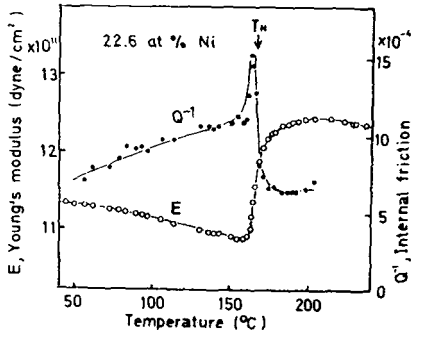

Fig.9 Temperature dependence of internal friction and Young's modulus of γ-phase alloy with 77.7 at%Mn and 22. 3at%Ni quenched from 950°C (9).

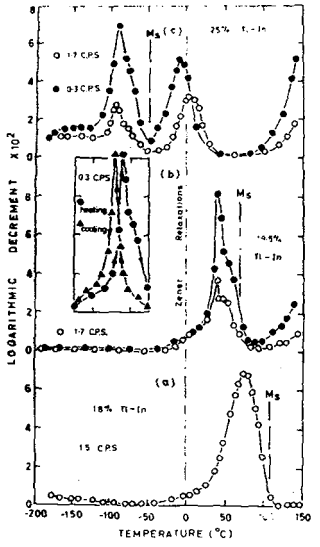

Fig.10 Internal friction peaks associated with the martensitic transformation and diffusion in single crystals of In-rich Tl alloys (10).

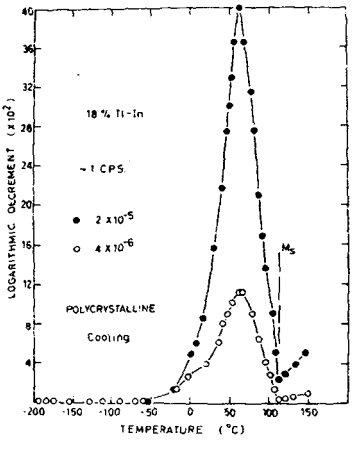

Fig.11 Effect of strain amplitude on internal friction in polycrystalline 18 at%Tl alloy (10).

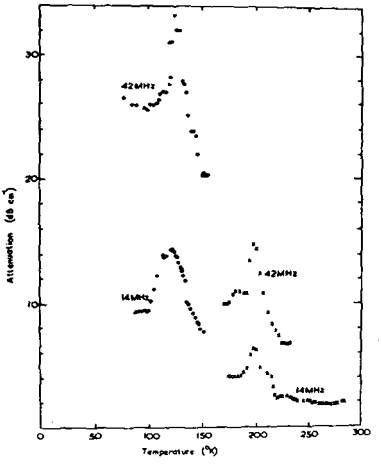

Fig.12 Ultrasonic attenuation peak associated with phase transformation in single crystals of In-Tl alloys (11).

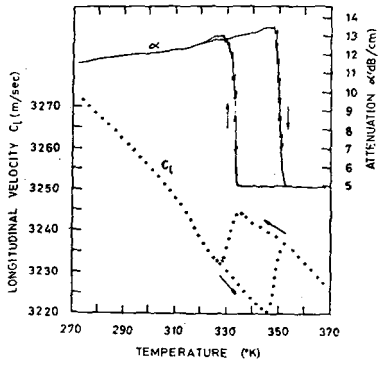

Fig.13 Temperature variation of the ultrasonic attenuation and sound velocity in Au-47.5 at%Cd alloy in the vicinity of cubic ⇌ orthorhombic phase transformation region (13).

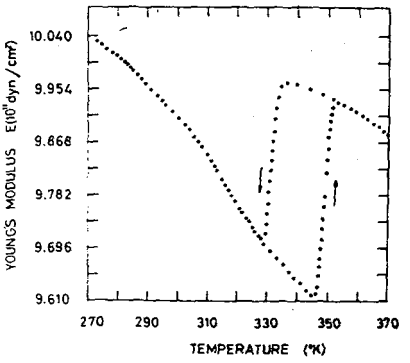

Fig.14 Temperature variation of Young's modulus in Au-47.5 at%Cd alloy in the cubic ⇌ orthorhombic phase transformation region (13).

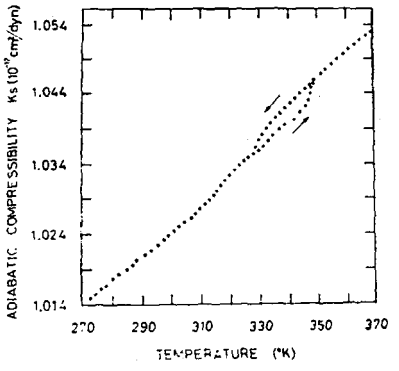

Fig.15 Temperature variation of the adiabatic compressibility in Au-47.5 at%Cd alloy in the cubic ⇌ orthorhombic phase transformation region(13).

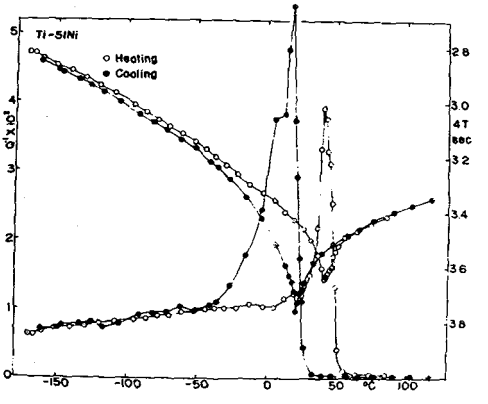

Fig.16 Internal friction and elastic modulus curves of a TiNi specimen annealed at 600°C for 2 hr and then furnace-cooled (14).

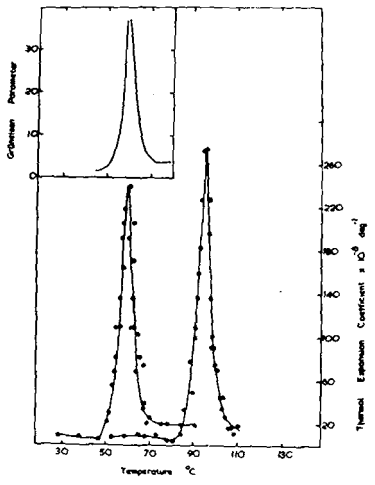

Fig.17 The linear thermal expansion coefficient of TiNi in the vicinity of the transition. The expansion maximum during heating occurs at a higher temperature than it does during cooling(15).

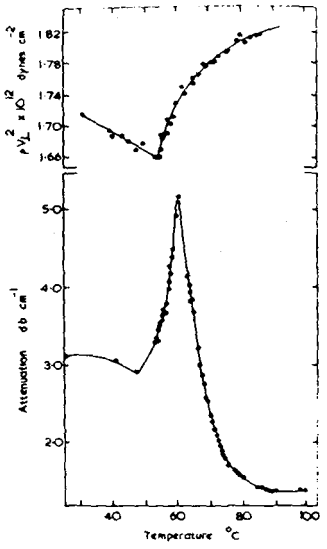

Fig.18 The temperature dependence in the vicinity of the transition of attenuation and velocity of longitudinal 15 MHz ultrasonic waves propagated through TiNi(15).

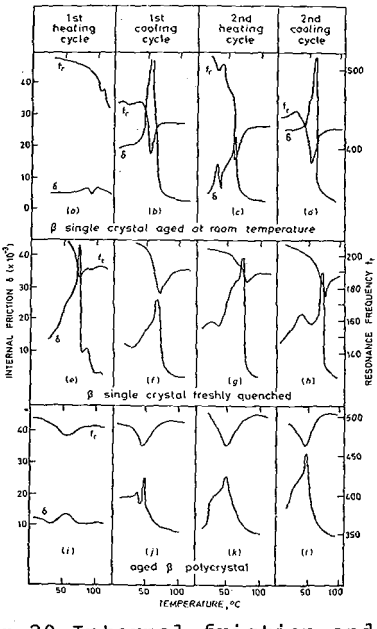

Fig.20 Internal friction and resonance frequency as a function of temperature in freshly quenched and aged specimens of βCu-Zn-Al alloys (20).

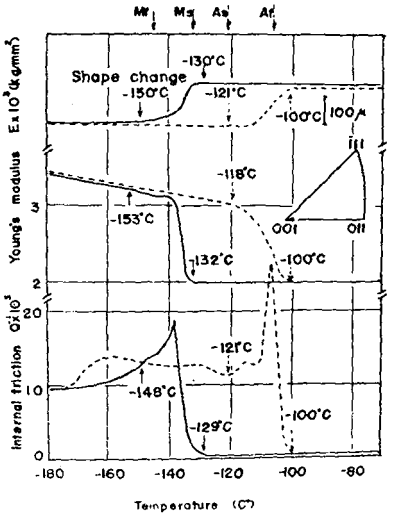

Fig.19 Simultaneous measurements of shape change, internal friction and Young's modulus during cooling (solid lines) and heating (dotted lines). See text for details (18).

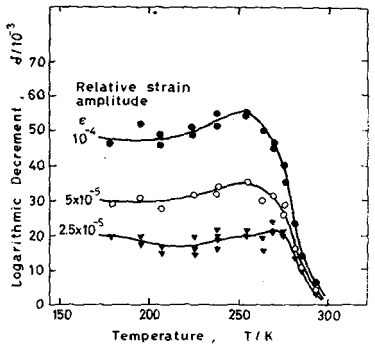

Fig.21 Internal friction spectrum obtained after 120 measuring oscillations during temperature steps. Frequency 1 Hz (21).

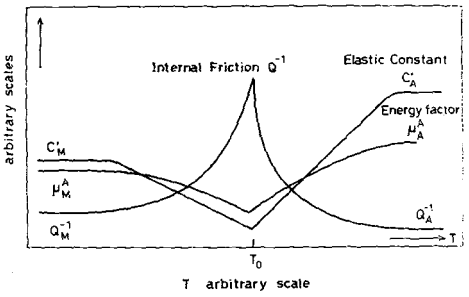

Fig.23 Schematic representation of the shear constant $C'=(C_{11}-C_{12})/2$, the energy factor μ and internal friction Q^{-1} as a function of temperature. The subscript M designates martensite and A austenite (25).

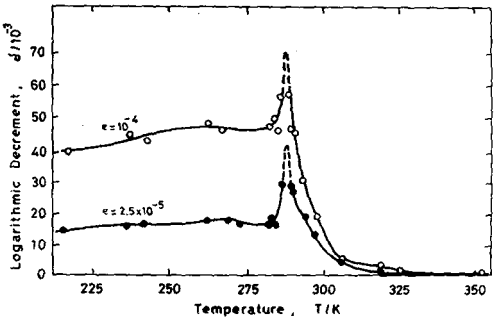

Fig.22 Internal friction spectrum obtained after 10 oscillations during constant temperature steps. Frequency 1 Hz (21).

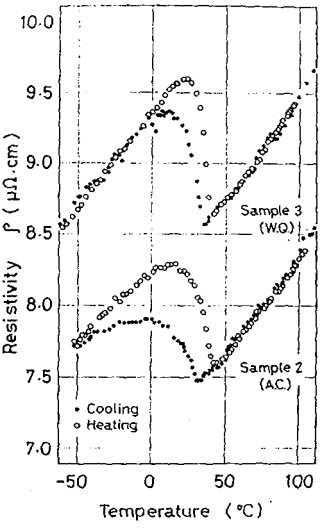

Fig.25 Effect of quenching rate on the change in resistivity with martensitic and reverse transformations in a Cu-26.00 wt%Zn-4.05 wt%Al alloy(22).

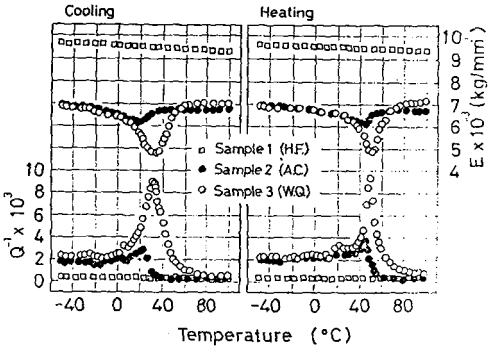

Fig.24 Effect of quenching rate on the internal friction and Young's modulus of a Cu-26.00 wt%Zn-4.05 wt%Al alloy. H.F.(hot forged and slow-cooled), A.C.(air-cooled), and W.Q.(water-quenched) (22).